Sensors Deployment Algorithms Under Limited Communication Range and Measurement Error

Hamid Mahboubi, Mojtaba Vaezi, and Fabrice Labeau
McGill University, Montreal, Quebec H3A 0E9, Canada

***Abstract*—We investigate mobile sensor deployment algorithms when the sensors have a limited communication range and they estimate other sensors location from the messages they receive from them. These pragmatic constraints bring two implications: the former implies that each sensor will only be aware of the presence of those sensors whose communication range includes that sensor, and the latter indicates that location information can be inaccurate, due to estimations error. Consequently, the conventional Voronoi-based mobile sensor deployment algorithms fail to guarantee a simple, reliable coverage detection; additionally, the sensors are prone to collision. We introduce a new set of Voronoi-based diagrams, named *guaranteed Voronoi diagrams with limited communication*, to tackle the above problems.**

***Index Terms*—Sensors deployment, coverage hole, guaranteed Voronoi diagram, estimation error, limited communication.**

I. Introduction

Mobile sensor networks (MSNs) are used for environmental sensing various applications [1]. Area coverage is a critical factor to fulfill the sensing tasks in many applications. Mobile sensors deployment algorithms are used to increase the total sensing coverage. They are particularly important when the network topology changes, as they are used to reduce the coverage holes, by adapting to the network topology. Significant topological changes can result simply from the malfunctioning of some sensor nodes, e.g., due to power failure [2].

To reduce the total *coverage hole*, movement-assisted sensor deployment protocols based on *Voronoi diagrams* are proposed both for the identical sensors [3]–[6] and non-identical sensors [7], [8]. Voronoi-based diagrams divide the field into regions, each corresponding to one sensor, such that: 1) these regions are *disjoint* 2) any point out of the *sensing disk* of one sensor, in its region, cannot be covered by other sensors and thus is a coverage hole. These two properties are very important in the sensor deployment algorithms. The former keeps the sensors away from collision and the latter makes it possible to evaluate the coverage of each region merely based on its own sensor.

The above diagrams, and corresponding deployment algorithms, assume that the exact location of all sensors are known at each node. However, this is not a realistic assumption, since each sensor usually estimates the location of its neighboring nodes by using a localization technique [9], [10], or it receives the location information by communication with them via a noisy communication channel [11]. In addition, it is assumed that the sensors's communication range is unlimited. Yet again, in practice this is not the case. These constraints affect the availability and accuracy of the location information of the sensors at each node, and degrades the performance of the system.

We investigate mobile sensor deployment algorithms with the following practical constraints: 1) the sensors' location information is not accurate, and 2) their communication range is limited. The effect of the first constraint, has already been studied by the authors in [12], [13], where *guaranteed Voronoi diagrams* are proposed to solve this problem. In this paper, we add the second constraint too.

Limited communication range in general can make a sensor oblivious to the presence of some sensors in the field. When unobserved sensors are among the neighbouring sensors of a sensor, the Voronoi region of that sensor will be expanded and may even include some of those unobserved sensors inside it. In such a case, the regions are no longer disjoint. This can reduce the total coverage of the network, since it increases the possibility of overlapping coverage areas. It also can result collision among sensors.

We introduce a set of new Voronoi-based diagrams that ensure disjoint regions for different sensor both when location information is not accurate and communication ranges are limited. The new diagrams are called *guaranteed Voronoi diagrams with limited communication*. While the proposed diagrams are competent in terms of final coverage, they incur more movements, yet with smaller strides, and they converge slower. These are due to the conservative partitioning we have adopted in order to prevent collision, if certain neighbouring sensors are not seen for their limited communication ranges.

This paper is organized as follows. We briefly review the weighted Voronoi-based diagrams in Section II, and introduce the proposed diagrams in Section III. We discuss the deployment algorithms in Section IV, and we present the numerical results in Section V. Section VI concludes the paper.

II. Definitions and Background

Let $\mathcal{F} \subset \mathbb{R}^2$ be a field containing n sensors s_i, $1 \leq i \leq n$, with sensing ranges r_i, $r_i > 0$, located at planar coordinate $p_i = (x_i, y_i)$. We denote this set of sensors by $\mathcal{S} = \{s_i\}$, where $i \in \mathcal{N} := \{1, 2, \ldots, n\}$. In this section, we assume $i, j \in \mathcal{N}$ and $i \neq j$, unless otherwise stated. We use $d(a, b)$ to denote the *Euclidean distance* between two points a and b. The *sensing disk* or *coverage area* of the sensor (s_i, r_i) is a *disk* of radius r_i centered at p_i, where p_i is the location of the sensor. Then, a point q is covered by this sensor if and only if $d(q, p_i) \leq r_i$, and the collection of all points in $\mathcal{F}$ that are out of the sensing circumcircles of all sensors is defined as *total*

coverage hole. If the sensing radii of the sensors are not the same, they are called *non-identical* sensors [14].

To be able to use a single-cell-based coverage hole detection in non-identical sensor networks, *weighted Voronoi diagrams* are proposed in the literature [8]. These diagrams are designed by modifying the distance metrics in a way that the distance metric depends on the sensing radii or the sensors, in addition to their distances. In the following, we list a few well-known weighted Voronoi diagrams and their corresponding regions.

1) Multiplicatively Weighted Voronoi Diagram (MWVD): In the MWVD, the set of all points q which are closer to the sensor s_i than to any other sensor in $\mathcal{F}$ is obtained by [12]

$$\Pi_i^{\mathrm{MWVD}} = \{q \in \mathcal{F} \mid \frac{d(q,p_i)}{r_i} \leq \frac{d(q,p_j)}{r_j}\}. \tag{1}$$

2) Additively Weighted Voronoi Diagram (AWVD): The AWVD divides the field $\mathcal{F}$ such that [13]

$$\Pi_i^{\mathrm{AWVD}} = \{q \in \mathcal{F} \mid d(q,p_i) - r_i \leq d(q,p_j) - r_j\}. \tag{2}$$

3) Power Diagram (PD): The power diagram partitions the field of sensors based in a way that the subregion corresponding to s_i is characterized by [12]:

$$\Pi_i^{\mathrm{PD}} = \{q \in \mathcal{F} \mid d^2(q,p_i) - r_i^2 \leq d^2(q,p_j) - r_j^2\}. \tag{3}$$

Note that, in all of the above weighted diagrams, for any $q \in \Pi_i$, we have $d(q,p_i) > r_i \Rightarrow d(q,p_j) > r_j$, meaning that if a point in Π_i is not covered by s_i it cannot be covered by any other sensor; i.e., the coverage holes can be found based on a *single-cell-based* search.

III. New Voronoi-Based Diagrams

A. Motivation

To construct its region, in a Voronoi based diagram, be it a standard or weighted Voronoi diagram, each sensor requires the locations of its neighboring sensors. If the location information is not communicated with a sensor or it is not perfect, the diagrams defined by (1)–(3) may not be disjoint and/or they cannot guarantee a single-cell-based coverage hole detection. A *disjoint* diagram is required to prevent collision between the sensors, and to limit the overlapping coverage, whereas a *single-cell-based* coverage detection algorithm simplifies the hole detection process and the development of distributed, self-deployment protocols for sensor networks. In this section, we generalize the above-mentioned weighted Voronoi diagrams and propose sensor deployment algorithms under the following practical constraints:

1) The location information of sensors is subject to error as the locations are estimated based on the messages each node receives from other nodes.
2) The communication range of sensors is limited and/or the link between them can be faulty, e.g., it may have excessive delay.

The objective is to find n subregions, each corresponding to one of the n sensors, such that it is guaranteed that

- If a point in a subregion is not sensed by its corresponding sensor, no other sensor can sense it either.
- These subregions are disjoint.

With perfect location information, both of the above conditions are easily satisfied for the standard or weighted Voronoi diagrams [3], [8]. However, with the above constraints neither of those objectives are necessarily satisfied in the conventional Voronoi diagrams. To tackle those constraints, we study sensor deployment problem under two assumptions: First, as proposed in [12], we assume that the estimation errors are upper bounded and these bounds are known at each sensor. Following the nomenclature of [12], let ϵ_{ij} denotes the maximum error in the estimation of the location of s_i at s_j. More precisely, assume that p_i, the exact location of s_i, be within a disk of radius ϵ_{ij}, $\epsilon_{ij} \geq 0$, centered at p_{ij}, where p_{ij} is the measured location of ith sensor at sensor j. Hence,

$$|d(q,p_i) - d(q,p_{ij})| \leq \epsilon_{ij}. \tag{4}$$

Likewise, suppose each sensor s_i measures its own location with some errors; this is represented by p_{ii} and the error bound is assumed to be ϵ_{ii}.

Second, we assume that sensor s_i can communicate (broadcast) its information within a radius of r_i^c. This range can be a fixed number for each type of sensors, for example, it may be a multiple of sensing radius. Let $r_{min}^c \triangleq \min\{r_1^c, r_2^c, \cdots, r_n^c\}$. Also, let $\mathcal{L}_i$ be the list of sensors whose messages reach the ith sensor. Mathematically, $\mathcal{L}_i \triangleq \{j \in \mathcal{N} \mid d(s_j,s_i) \leq r_j^c\}$. We will use this definition in the region construction, as explained in the following.

B. Regions' Characteristics

In view of the constraints we mentioned previously, in this section, we modify the weighted Voronoi diagrams such that the new diagrams ensure a single-cell-based search for coverage holes detection, within each cell. The new diagrams must be reliable both in the presence of estimation errors and limited communication between the sensors. It is worth mentioning that, without the second constraint the information of all sensors could be potentially used in the region construction for one sensor. However, when the second constraint comes in, this list is reduced to $\mathcal{L}_i$ since the messages of the remaining sensors are not reached to s_i and thus cannot be used. Then, since we are considering both constraints concurrently, the list of potential neighbours is limited to $\mathcal{L}_i$.

To tackle the first constraint, note that, if p_{ij} is the estimated position of the ith sensor at sensor j for any $i,j \in \mathcal{N}$, then the exact location of s_i (denoted by p_i) is somewhere within a disk of radius ϵ_{ij} centered at p_{ij}. Thus, for an arbitrary distance function f, the set of all points $q \in \mathcal{F}$ surely closer to s_i than to s_j is characterized by [12]

$$\max_{q_1 \in \mathrm{C}(p_{ii},\epsilon_{ii})} f(q,q_1,r_i) \leq \min_{q_2 \in \mathrm{C}(p_{ji},\epsilon_{ji})} f(q,q_2,r_j) \quad \forall j \in \mathcal{L}_i, \tag{5}$$

where $\mathrm{C}(a,r)$ represents a circle of radius r centered at a. In Table I, we list the distance function f for certain well-known weighted distances, used in the sensor network literature.

This formulation per se does not guarantee a disjoint region for each sensor in the case of faulty or limited communication, because when some sensors are not able to communicate with a given sensor, the region identified for that sensor can be, in

TABLE I
DISTANCE FUNCTION ($f(q, q_1, r_i)$) AND BORDER SHAPE FOR CERTAIN WEIGHTED VORONOI DIAGRAMS

Diagram Type	Distance function	Borders
MWVD	$\frac{d(q,q_1)}{r_i}$	circular arc
AWVD	$d(q, q_1) - r_i$	hyperbolic arc
PD	$d^2(q, q_1) - r_i^2$	line

general, greater than that when they all communicate. Hence, we need to address this issue as well. To this end, for any $i \in \mathcal{N}$, it suffices to have

$$\max_{q_3 \in \mathrm{C}(p_{ii}, \epsilon_{ii})} d(q, q_3) \leq \frac{r_{\min}}{2} \quad \forall j \in \mathcal{L}_i. \tag{6}$$

Specifically, we can write

$$d(q, p_{ii}) \leq \frac{r_{\min}}{2} - \epsilon_{ii} \quad \forall j \in \mathcal{L}_i. \tag{7}$$

Proposition 1. *The regions defined by* (5)-(6) *are disjoint.*

Proof. If s_i and s_j are able to communicate, then from (5) we know that Π_i and Π_j are disjoint (they are subsets of two disjoint regions, and thus they are disjoint). On the other hand, if s_i and s_j are not able to communicate then, by definition, $d(p_i, p_j) > r_{\min}$. Under such a circumstance, (6) guarantees Π_i and Π_j to be disjoint. To prove this, assume that, for contradiction, a point q belongs to both regions. Then, from (6) we get

$$q \in \Pi_i \Rightarrow d(q, p_{ii}) \leq \frac{r_{\min}}{2} - \epsilon_{ii}, \tag{8a}$$

$$q \in \Pi_j \Rightarrow d(q, p_{jj}) \leq \frac{r_{\min}}{2} - \epsilon_{jj}, \tag{8b}$$

and, we can write:

$$\begin{aligned} d(p_i, p_j) &\leq d(p_i, p_{ii}) + d(p_{ii}, p_{jj}) + d(p_{jj}, p_j) \\ &\leq d(p_{ii}, p_{jj}) + \epsilon_{ii} + \epsilon_{jj} \\ &\leq d(q, p_{ii}) + d(q, p_{jj}) + \epsilon_{ii} + \epsilon_{jj} \\ &\leq r_{\min} \end{aligned}$$

where the first and third inequalities follow from the *triangle inequality*, the second inequality follows from the fact that p_i and p_j, respectively, are within disks of radius ϵ_{ii} and ϵ_{jj} centered at p_{ii} and p_{jj}, and the last inequality follows from (8a) and (8b).

Obviously, this is contradicting as it implies that s_i and s_j are able to communicate. Therefore, in any cases the regions defined by (5) and (6) are disjoint. □

In the reminder of this section, we characterize the region corresponding to weighted distances listed in Table I. We basically simplify (5) using different distance functions and noting that the maximum possible distance between q and a point in $\mathrm{C}(p_{ii}, \epsilon_{ii})$ is $d(q, p_{ii}) + \epsilon_{ii}$ and the minimum distance between q and a point in $\mathrm{C}(p_{ji}, \epsilon_{ji})$ is $d(q, p_{ji}) - \epsilon_{ji}$. We will use them to find the cell borders.

Using such a modified diagram, it is guaranteed that, even in the presence of the location estimation error and limited communication range, a point inside a subregion can only be sensed by its corresponding sensor. To find the mathematical characterization of the ith region for different weighted diagrams under limited communication condition we just need to apply the corresponding distance function from Table I to (5) and incorporate (6), or equivalently (7).

1) Guaranteed Multiplicatively Weighted Voronoi Diagram with Limited Communication (GMWVD-LC):

$$\begin{aligned} \Pi_i = \{q \in \mathcal{F} \mid \frac{d(q, p_{ii}) + \epsilon_{ii}}{r_i} \leq \frac{d(q, p_{ij}) - \epsilon_{ij}}{r_j}, \\ d(q, p_{ii}) \leq \frac{r_{\min}}{2} - \epsilon_{ii} \quad \forall j \in \mathcal{L}_i\}. \end{aligned} \tag{9}$$

The two constraint can be absorbed in one constraint as

$$\frac{d(q, p_{ii}) + \epsilon_{ii}}{r_i} \leq \min\{\frac{d(q, p_{ij}) - \epsilon_{ij}}{r_j}, \frac{r_{\min}}{2r_i}\}.$$

2) Guaranteed Additively Weighted Voronoi Diagram with Limited Communication (GAWVD-LC):

$$\begin{aligned} \Pi_i = \{q \in \mathcal{F} \mid d(q, p_{ii}) \leq \frac{r_{\min}}{2} - \epsilon_{ii}, \\ d(q, p_{ii}) - r_i + \epsilon_{ii} \leq d(q, p_{ij}) - r_j - \epsilon_{ij}\}. \end{aligned} \tag{10}$$

Again, the two constraint can be simplified as

$$d(q, p_{ii}) - r_i + \epsilon_{ii} \leq \min\{d(q, p_{ij}) - r_j - \epsilon_{ij}, \frac{r_{\min}}{2} - r_i\}.$$

3) Guaranteed Power Diagram with Limited Communication (GPD-LC):

$$\begin{aligned} \Pi_i = \{q \in \mathcal{F} \mid [d(q, p_{ii}) + \epsilon_{ii}]^2 - r_i^2 \leq [d(q, p_{ij}) - \epsilon_{ij}]^2 - r_j^2, \\ d(q, p_{ii}) \leq \frac{r_{\min}^2}{2} - \epsilon_{ii} \quad \forall j \in \mathcal{L}_i\}. \end{aligned} \tag{11}$$

Remark 1. One special case of the above diagrams is the case where $r_{\min} \to \infty$, i.e., the is no communication limit. If so, the above regions become the same as the regions in [12].

C. Regions' Properties

One fundamental property of the above diagrams is that if a point in Π_i is not covered by s_i it cannot be covered by any other sensor. That is, the coverage holes can be found on a *single-cell-based* search. This is because

Property 1. In all of the above diagrams, for any $q \in \Pi_i$, $d(q, p_i) > r_i \Rightarrow d(q, p_j) > r_j$.

We should remind that Proposition 1 is valid also for any of the above guaranteed regions. Therefore,

Property 2. the regions defined by (9)–(11) are disjoint.

The proposed diagrams are designed in a way that each sensor can move only inside its associated region. Hence, the sensors are prevented to enter other sensors region and are not prone to collision. Collision avoidance is very important in the context of managing multiple vehicles, including mobile sensor networks.

Property 3. The regions defined by the diagrams in (9)–(11) do not partition the field, i.e., $\bigcup_{i=1}^{n} \Pi_i \neq \mathcal{F}$

This property is similar to that of the weighted diagrams, and implies that with the above partitioning, there will be some *neutral areas* in the field which do not belong to any of

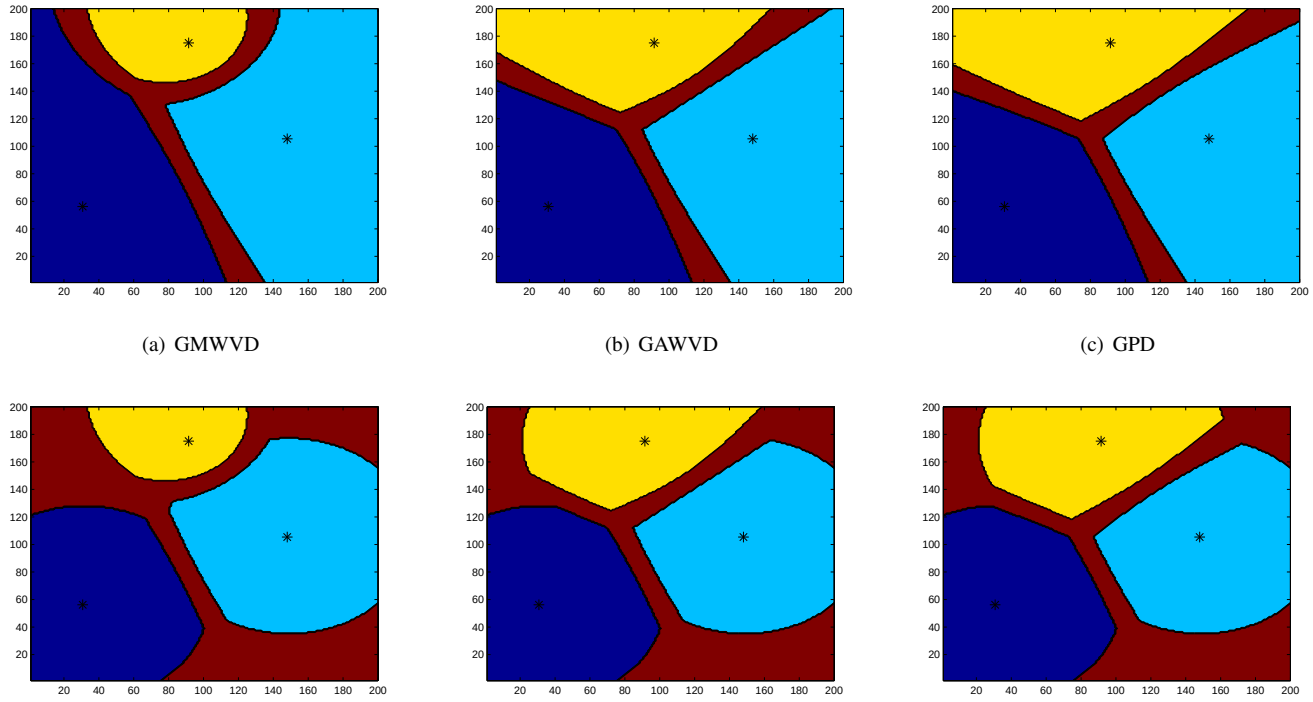

(a) GMWVD (b) GAWVD (c) GPD

(d) GMWVD-LC (e) GAWVD-LC (f) GPD-LC

Fig. 1. Guaranteed diagrams for a field containing three sensors with different sensing radii and imperfect location information, for different algorithms. In Figs. 1(a)-1(c) the sensors' communication range is unlimited, while in Figs. 1(d)-1(f) it is limited. The regions in dark brown are the areas which are not assigned to any sensor, implying that a single-cell-based coverage hole detection is not applicable to them.

the guaranteed regions. observe that the neutral areas are not necessarily coverage holes; they can be covered with one or more sensors. Examples of the above-mentioned guaranteed diagrams, both with limited and unlimited communication ranges, are shown in Fig. 1, where it is obvious that properties 2 and 3 hold. The sensing range of sensors are 6m, 6m and 3m, and their communication ranges are 12.5 times of the sensing ranges, and ϵ_{ii} and ϵ_{ij} are 1m and 2m, respectively.

IV. Deployment Protocols

The deployment algorithm and movement strategies used in this paper are exactly the same as those in [12], except that the minimum communication range of the network is exposed to all sensors. We briefly mention them here; further details can be found in [12].

A. Deployment Algorithm

The proposed deployment algorithms are iterative, and include the following steps are in each iteration:

i) All sensors broadcast their sensing radii and positions. Besides, we assume that all sensors are exposed to the minimum communication range ($r_{\min}$) of the network. According to the received information, and the characteristics of the region to be build, every sensor constructs its own region.

ii) Each sensor independently detects coverage holes in its region.

iii) If coverage holes are found in any regions, the corresponding sensors calculate their new candidate location, by using a specific movement algorithm (which will be discussed in subsection IV-B).

iv) Once the new locations are calculated for each sensor, the corresponding coverage areas is evaluated and compared to the current coverage area. Only the sensors whose new coverage areas are greater than their present value move to their new locations; other sensors do not move in this iteration.

v) The algorithm is terminated in the iteration where no sensor can improve its coverage area by predefined threshold (δ) or when a predefined number of iterations ($I_{\max}$) has been completed.

B. Movement Strategies

A movement strategy is required in step iii of the above algorithm to determine the new candidate point (position) for each sensor. We use the following strategies in our work:

1) Farthest Point (FP) Strategy: This moves every sensor to the farthest point in its region in hope of reducing the area of coverage hole.

2) Minmax Point (MP) Strategy: For certain network topologies and sensor configurations, e.g., regions with very acute angle, the FP strategy may not be very effective. To achieve maximum coverage, the minmax point (MP) strategy minimizes the maximum distance of the sensor from any point in its corresponding region.

These two movement strategies can be used in combination with the diagrams we introduced in Section III. Therefore, in

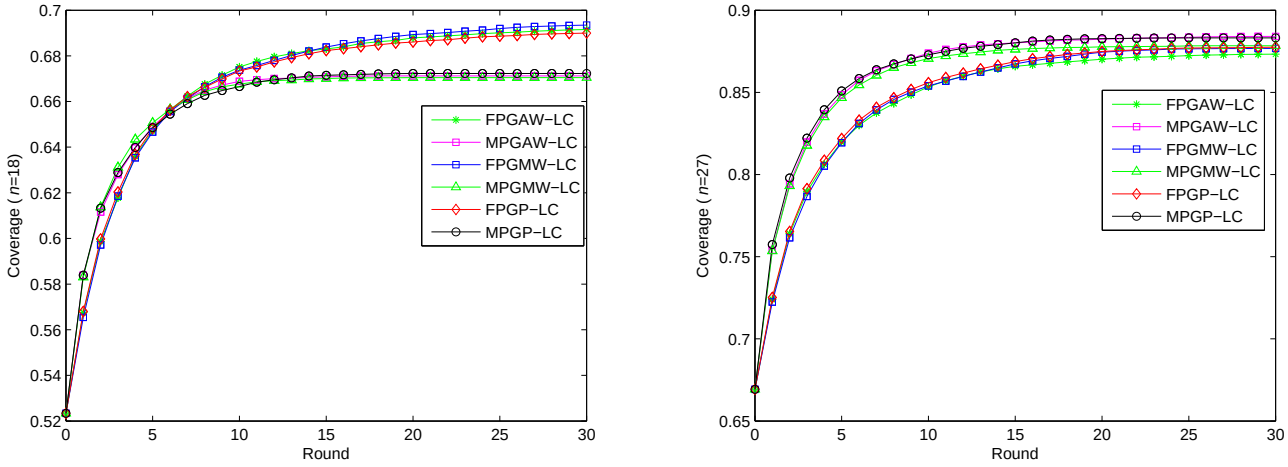

(a) (b)

Fig. 2. Network coverage using different algorithms at various iterations: (a) for 18 sensors (b) for 27 sensors.

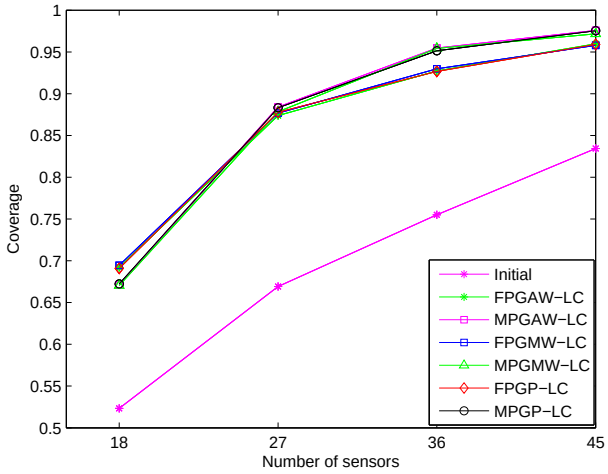

Fig. 3. Initial and final coverage versus the number of sensors for different algorithms. The FP- and MP-based algorithms make two separate clusters, and within each cluster there is not much difference between the final coverage.

total, six deployment algorithms are possible. Specifically, if the FP strategy is used for movement (step iii of the above iterative algorithm), we we can have

- Farthest point based GMWVD-LC (FPGMW-LC)
- Farthest point based GAWVD-LC (FPGAW-LC)
- Farthest point based GPVD-LC (FPGP-LC)

Similarly, one can use the MP movement strategy in each of the diagrams to get MPGMW-LC, MPGAW-LC and MPGP-LC deployment algorithms. We compare the performance of these algorithms in the next section.

V. Simulation Results

To evaluate the performance of the proposed algorithms, we run simulations for various number of sensors in a 50m $\times$ 50m field. We use three types of sensors with sensing radii equal to 5m, 6m, and 7m. Table II shows the number of sensors from each type for different n. For each n, we carry out simulations using all of the six algorithms we developed, namely the FPGAW-LC, FPGMW-LC, FPGP-LC, MPGAW-LC, MPGMW-LC, and MPGP-LC. The results are obtained by using 20 random initial arrangements for the sensors. The coverage improvement threshold δ is set to be $0.1m^2$, meaning that the algorithm stops if the local coverage improvement by all sensors is less than $0.1m^2$. For all nodes, ϵ_{ii} and ϵ_{ij} are set 0 and 1m, respectively.

TABLE II
The number of sensors and their radii for each n.

	$r = 5m$	$r = 6m$	$r = 7m$
$n = 18$	6	8	4
$n = 27$	9	12	6
$n = 36$	12	16	8
$n = 45$	15	20	10

Total sensing coverage of the field is often the most important performance indicator. We present it in Fig. 2 where the ratio of the covered area to the total area versus the number of iterations are plotted when 18 and 27 sensors are deployed in the field. It can be seen that the coverage increment is sharp for the first several iterations and reduces later. As expected, the sensing coverage depends on the number of sensors and it increases with n. To see this, we plot the initial and final coverage factor versus the number of sensors in Fig. 3.

The coverage provided by the MP-based algorithms is larger than that of the FP-based algorithms, in general. The FP-based algorithms are however more energy-efficient than the MP-based ones. Energy consumption in sensor deployment mainly depends on three parameters [15], [16]: number of movements (starting/braking), travel distances, and number of iterations to reach the termination condition. These three parameters

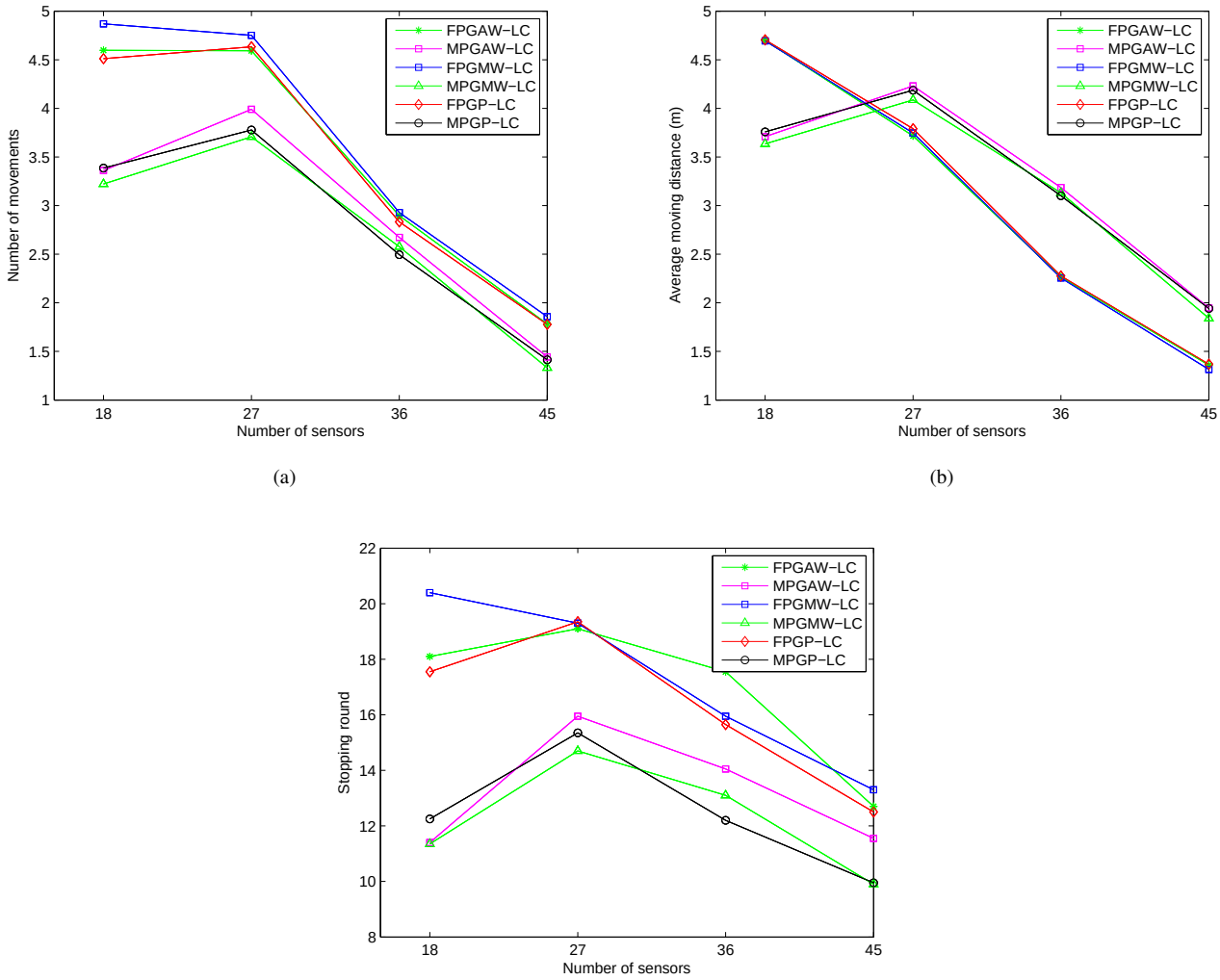

Fig. 4. Movement related graphs for the proposed algorithms with different number of sensors: (a) number of movements, (b) average travel distance per sensor, and (c) average number of iterations, required to reach the termination condition.

are shown in Fig. 4, respectively. Figure 4(a) represents the average moving distance per sensor, required to cover the field, which decreases as n goes up. This is because, the higher the number of sensors, the better the initial coverage and thus fewer movements are needed to improve the coverage.

A key observation from Figs. 2–4 is that the performance of the MP-based algorithms is somewhat the same, in terms of coverage, moving distance, number of movements to achieve a certain level of coverage, and the energy required for that. Similarly, the FP-based algorithms behave almost the same. Hence, in light of these results, we draw the conclusion that, the structure of the cells in the GAWVD-LC, GMWVD-LC and GPD-LC diagrams, does not have a big impact on the performance of the deployment algorithms. In contrast, the movement strategy (FP or MP) is determinant, as for a given diagram (e.g., the GPD-LC), the performance of the deployment algorithms is noticeably different for the MP- and FP-based strategies.

Finally, to understand the effect of the limited communication ranges, we compare the results of this paper with those of [12]. As we mentioned in Section III, the proposed diagrams in (9)–(11) reduces to the corresponding diagrams in [12] when the communications ranges are unlimited ($r_{\min} \to \infty$). Thus, the difference between the two set of result must be due to the limited communication range, or equivalently, due to the difference in the corresponding diagrams. These differences can be summarized as:

1) When there is no limit on the communication ranges, the coverage reaches to its steady state much faster, i.e., the convergence time is less the case with limited communication ranges.
2) The number of movements and the average number of iterations to reach the termination condition, in the diagrams proposed in this paper are nearly twice of those in [12] where there was no limit on the communication ranges.
3) The average moving distances do not differ much.

These observations make sense as we have chosen a more

conservative approach for region construction. As we can see from Fig. 1, in all three diagrams, the regions belonging to the sensors have shrunk due to the conservative way we have modeled the limit on the communication ranges. Hence, the distances of sensors to the corners of their regions has become less. Consequently, both the farthest point and minmax point strategies result in smaller strides in each movement, compared to what they would have given with no limit. Therefore, the coverage increment at each movement is less than it would be. That is, the sensors tend to move more often, but in smaller strides. It is worth noting that, although the average traveled distances are not changed noticeably, the energy consumption is expected to increase due to the limited communication ranges. This is because each starting/braking consumes energy.

VI. Conclusions

We have introduced a collection of new diagrams for mobile sensor networks with non-identical sensors, in the presence of location estimation errors and when the communication ranges the sensors are limited. These diagrams are designed in a way that the search for local coverage holes is performed independently in each cell, and thus is simple. Besides, the boundaries of the sensors regions are separate which reduce the chance of overlapping coverage areas. Simulation results show that the proposed diagrams and deployment algorithms increase the network's coverage even in the presence of the above constraints. Compared to the case where there is no constraint on the communication range, the proposed diagrams converge slowly and require more stopping/barking, but their final coverage is as good as them.

References

[1] I. F. Akyildiz, W. Su, Y. Sankarasubramaniam, and E. Cayirci, "A survey on sensor networks," *IEEE Communications Magazine*, vol. 40, no. 8, pp. 102–114, 2002.

[2] J. N. Al-Karaki and A. E. Kamal, "Routing techniques in wireless sensor networks: a survey," *IEEE Wireless communications*, vol. 11, no. 6, pp. 6–28, 2004.

[3] G. Wang, G. Cao, and T. La Porta, "Movement-assisted sensor deployment," *IEEE Transactions on Mobile Computing*, vol. 5, no. 6, pp. 640–652, 2006.

[4] S. Megerian, F. Koushanfar, M. Potkonjak, and M. B. Srivastava, "Worst and best-case coverage in sensor networks," *IEEE Transactions on Mobile Computing*, vol. 4, no. 1, pp. 84–92, 2005.

[5] Q. Du, V. Faber, and M. Gunzburger, "Centroidal Voronoi tessellations: Applications and algorithms," *SIAM review*, vol. 41, no. 4, pp. 637–676, 1999.

[6] J. Cortes, S. Martinez, T. Karatas, and F. Bullo, "Coverage control for mobile sensing networks," in *Proc. IEEE International Conference on Robotics and Automation (ICRA)*, vol. 2, pp. 1327–1332, 2002.

[7] H. Mahboubi, J. Habibi, A. Aghdam, and K. Sayrafian-Pour, "Distributed deployment strategies for improved coverage in a network of mobile sensors with prioritized sensing field," *IEEE Transactions on Industrial Informatics*, vol. 9, no. 1, pp. 451–461, 2013.

[8] H. Mahboubi, K. Moezzi, A. G. Aghdam, and K. Sayrafian-Pour, "Distributed deployment algorithms for efficient coverage in a network of mobile sensors with nonidentical sensing capabilities," *IEEE Transactions on Vehicular Technology*, vol. 63, no. 8, pp. 3998–4016, 2014.

[9] L. Hu and D. Evans, "Localization for mobile sensor networks," in *Proceedings of the 10th annual international conference on Mobile computing and networking*, pp. 45–57, ACM, 2004.

[10] G. Han, H. Xu, T. Q. Duong, J. Jiang, and T. Hara, "Localization algorithms of wireless sensor networks: a survey," *Telecommunication Systems*, vol. 52, no. 4, pp. 2419–2436, 2013.

[11] F. Sharifi, Y. Zhang, and A. Aghdam, "A distributed deployment strategy for multi-agent systems subject to health degradation and communication delays," *Journal of Intelligent & Robotic Systems*, vol. 73, no. 1-4, pp. 623–633, 2014.

[12] H. Mahboubi, M. Vaezi, and F. Labeau, "Mobile sensors deployment subject to measurement error," in *Proc. VTC Fall*, pp. 1–5, 2014.

[13] H. Mahboubi, M. Vaezi, and F. Labeau, "Distributed deployment algorithms in a network of nonidentical mobile sensors subject to location estimation error," in *Proc. IEEE Sensors*, 2014.

[14] X. Wang, S. Han, Y. Wu, and X. Wang, "Coverage and energy consumption control in mobile heterogeneous wireless sensor networks," *IEEE Transactions on Automatic Control*, vol. 58, no. 4, pp. 975–988, 2013.

[15] S. Yoon, O. Soysal, M. Demirbas, and C. Qiao, "Coordinated locomotion and monitoring using autonomous mobile sensor nodes," *IEEE Transactions on Parallel and Distributed Systems*, vol. 22, no. 10, pp. 1742–1756, 2011.

[16] H. Mahboubi, K. Moezzi, A. G. Aghdam, K. Sayrafian-Pour, and V. Marbukh, "Distributed deployment algorithms for improved coverage in a network of wireless mobile sensors," *IEEE Transactions on Industrial Informatics*, vol. 10, no. 1, pp. 163–174, 2014.